Characterization of Hybrid ^{3}He Cells Using NMR

A thesis submitted in partial fulfillment of the requirement
for the degree of Bachelor of Science with Honors in
Physics from the College of William and Mary in Virginia,

by

Paul J. Black

Accepted for _____
(Honors)

_____
Advisor: Dr. Todd Averett

_____
Dr. Gina Hoatson

_____
Dr. Gunter Luepke

Williamsburg, Virginia
May 2007

I would like to thank my advisor, Dr. Todd Averett for his continuous help, patience, and motivation. I would also like to thank Sabine Fuchs, who was invaluable in teaching me about the lab, as well as providing help whenever it was needed. I would like to thank Klaus Grimm for taking the time to help me with aspects of the project. Finally, I would like to thank Jaideep Singh, who greatly helped me to understand difficult concepts in gaussian optics.

Abstract

This project involves modifying and calibrating many of the components used to measure specific characteristics of polarized ^{3}He cells to accommodate a new glass cell design with a higher volume and hybrid mixture of Potassium(K) and Rubidium(Rb). The work put into this project went in two major directions. The first was an attempt at establishing an in house method for measuring the density of a filled ^{3}He cell. The second direction in this project is to redesign and calibrate a new target oven and NMR system which will be utilized to measure the effective polarization of the target cells that will be used in conjunction with the electron beam at Jefferson Lab for upcoming experiments.

Contents

List of Figures

1 Introduction

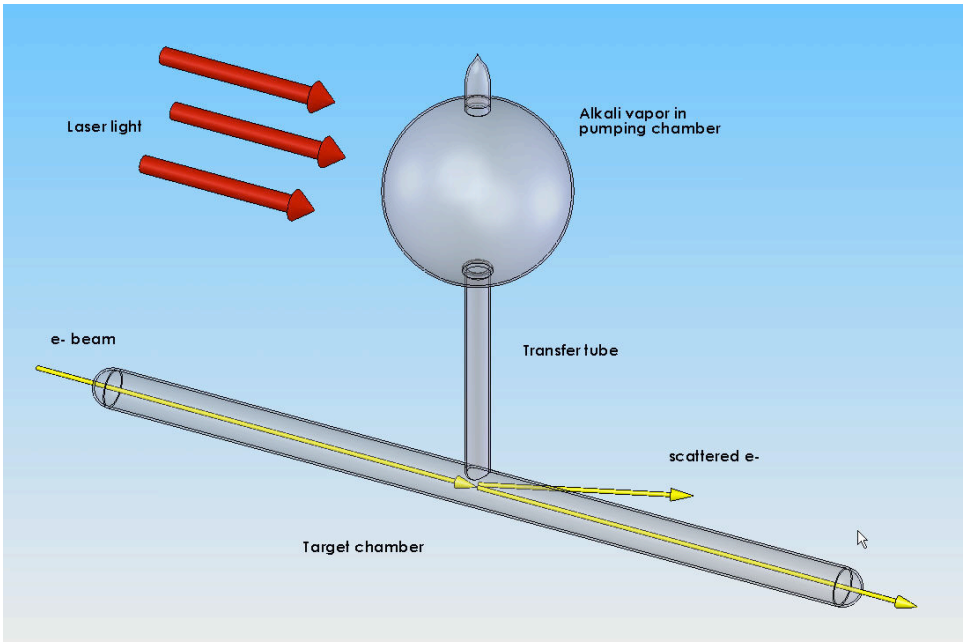

Figure 1: This is the basic design of all polarized ^{3}He target cells. The optical pumping occurs in the spherical bulb at the top of the cell. The pumping chamber contains Rb and K which is vaporized for the optical pumping process. The long cylindrical chamber, known as the target chamber contains primarily ^{3}He and N_2. At Jefferson lab an electron beam is directed into the target chamber.[3]

Polarized ^{3}He targets are used in conjunction with electron scattering measurements at the Thomas Jefferson National Accelerator Facility (Jefferson Lab) to investigate the properties of the neutron. The most likely configuration of the ^{3}He nucleus contributes mostly neutron spin to the total spin of the nucleus. This means that polarized ^{3}He nuclei provide a stable source of polarized neutrons used to study the neutron spin at Jefferson Lab[4].

The measurements performed at Jefferson Lab require accurate knowledge of the density of the gas within the target cell. The value of density is currently calculated

by measuring the pressure of the ^{3}He cell before it is sealed and then applying the ideal gas law to solve for the density. Pressure broadening can be used to determine the density of the gas within the cell after it has been sealed. This concept involves the broadening of the atomic absorption lines unique to every element due to the kinetic interactions between the element in question and the surrounding gas. Using a pressure broadening technique to determine the density of gas within a cell could reduce the error in measurements done at Jefferson Lab. The first direction of this project was to investigate the possibility of converting the laser used in the lab for optical pumping into a fine-tunable laser for the purpose of building a new system for measuring the density of gas within the new target cells.

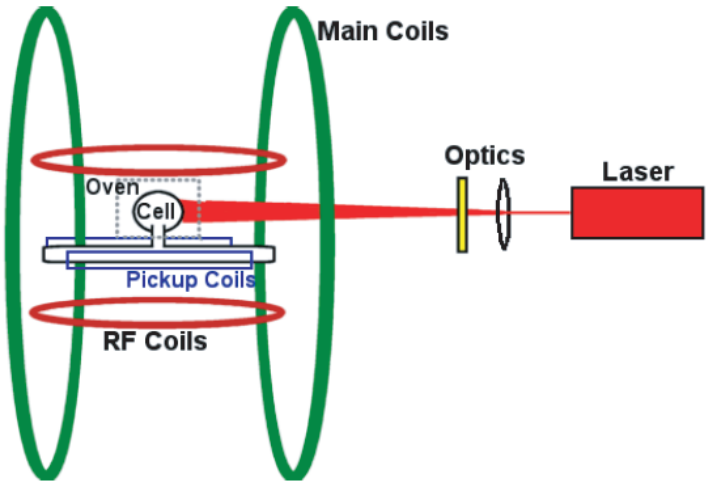

Figure 2: This is the apparatus used for polarization and polarimetry of ^{3}He. The main coils, laser, oven, and optics are used to polarize ^{3}He via optical pumping. The main coils, RF coils, and pickup coils are used as an NMR apparatus to measure polarimetry.[4]

The lab used to fill target cells at William and Mary has begun to use a new type of glass cell with a larger volume and two alkali species, Potassium(K) and

Rubidium(Rb). The new cell design requires a new oven and NMR system to be designed to do the polarization and polarization measurements of ^{3}He gas. The second direction of this project is to redesign and build a new polarization and NMR apparatus to accommodate the new cell design. When completed, this system will be used to polarize ^{3}He cells filled in house and measure the polarization of the ^{3}He after the process. If time allows, the polarization process will be optimized in order to reduce error.

2 Theory

2.1 Gaussian Optics

The topic of gaussian optics became critical to the first direction of this project. The laser system available for use in density measurements had a gaussian profile when emitted from the fiber. In order to convert this output to a low divergent, narrow beam, the behavior of gaussian optics had to be well understood. The following equation fully describes the power as a function of radius and z, the axis of propagation:

$$P(r,z) = \frac{\pi}{4}\sqrt{\frac{\epsilon}{\mu}}E_0^2(z)\omega^2(z)\left[1-\exp\left(-2\frac{r^2}{\omega^2(z)}\right)\right] \tag{1}$$

Where $\mathrm{E}_0(z)$ is the magnitude of the polarization vector as a function of z, the axis of propagation, ϵ and μ are the electric permittivity and magnetic permeability of the medium respectively, and $\omega(z)$ is the beam radius as a function of z. Conservation of energy can be used to treat the terms outside of the brackets as a constant. The power passing through a plane perpendicular to the axis of propagation must remain constant. This eliminates the z dependence on power, so long as we are dealing with it one plane at a time along the axis of propagation.[8] Unlike traditional optics, in which light emitted from a fiber expands linearly with distance, gaussian beams expand like a gaussian function. At or near the fiber tip, we can find the beam waist.

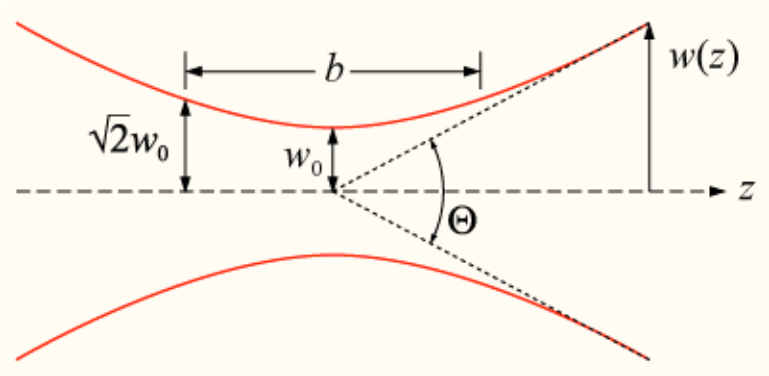

Figure 3: This figure illustrates the behavior of a typical gaussian beam along the axis of propagation z. The beam waist is represented by ω_0 while the far field divergence is represented by Θ. It is clear from this illustration that the expansion of the gaussian wave attains a linear dependence as z becomes sufficiently large.[1]

This is the point at which the laser light has a minimum diameter. The divergence of a gaussian beam is not constant with increasing distance from the source[5]. The divergence does, however, approach a linear dependence at a large distance. This behavior is illustrated in Figure 3. This is why the divergence of a gaussian beam is referred to as the far field divergence; The beam waist and far field divergence are directly proportional to each other given by the invariant:

$$\alpha = \Theta\omega_0 \tag{2}$$

Where α is a constant given by the relation:

$$\alpha = M^2\frac{\lambda}{\pi} \tag{3}$$

In this equation, the constant M^2 is a constant that represents the deviation from an ideal gaussian beam[8]. Since this factor must be found empirically, it is usually sufficient to empirically solve for the constant α. This invariant relates the beam waist radius, ω_0 and the far field divergence, Θ. The goal in the initial aim of the

project was to create a system in which the beam waist and far field divergence were minimized. When simple spherical optics are used to manipulate light with a gaussian

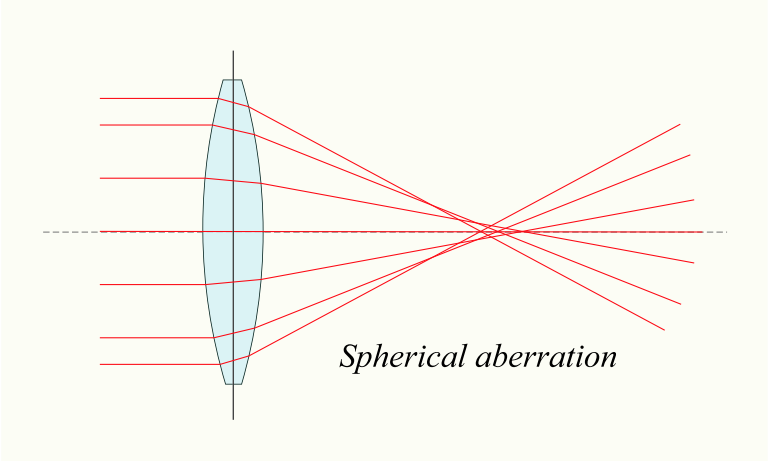

Figure 4: This figure illustrates the effect of spherical aberrations. Instead of light being converged to a single point, the effect causes a blurred focus. This adds to the problem of a large beamspot and makes the minimum focus permitted by geometric manipulations in optics difficult.[2]

profile, spherical aberrations introduce a stronger dependence between the beam waist and the far field divergence. In other words, spherical aberrations increase α in the invariant given by Equation 19. Spherical aberrations occur when light is incident on a spherical lens with imperfections in the geometry or material of the lens. Spherical aberrations prevent a lens from focusing light incident on it to a point. This effect is illustrated in Figure 4.

2.2 Pressure Broadening

Every element and molecule has an inherent theoretical absorption spectra unique to the probable quantum mechanical energy transitions of the subatomic particle that comprise each molecule. The spectra consists of a series of absorption lines, each

corresponding to a photon of a particular energy equal to the transition energy of an electron within the molecule. Photons of energy equal to a transition energy will be absorbed. The energy of the photon is directly proportional to its frequency. If a tunable laser with a range containing an absorption frequency is directed into a gas and the laser is tuned through a range of frequencies, including the absorption frequency, the absorption curve given by the spectrometer will look much like a Dirac Delta function centered at the absorption frequency. This absorption distribution will change if affected by pressure broadening.

The concept of pressure broadening involves the kinetic interactions between molecules in a nonuniform gas. The added energy of kinetic interactions between molecules cause a broadening effect of the absorption lines. This broadening changes the typical Dirac Delta function normally associated with photon absorption to a Lorentzian distribution. The model for a Lorentz function used to fit absorption data of this nature is given by Equation 4:

$$R(\nu) \equiv \frac{A[1 + 0.6642 \cdot 2\pi \cdot T_d(\nu - \nu_c)]}{(\nu - \nu_c)^2 + (\frac{\gamma}{2})^2} + B \tag{4}$$

Where A, T_d, ν_c, γ, and B are fitting parameters used to minimize the error involved. The parameter γ, which fits the linewidth of the absorption curve is directly proportional to the number density of helium(n_b) by the relation $\gamma = \Gamma n_b$[6]. The parameter Γ is known as the broadening coefficient. This coefficient was calculated to great accuracy in a different study. The value of Γ will be used to calculate the number density of the ^{3}He in the cell.[6]

2.3 Circular Polarization and Angular Momentum

In order to achieve a net polarization of ^{3}He, angular momentum must be transferred from incident photons. In order to achieve this, polarization of laser light must be circular. The polarization of any electromagnetic wave is describable in terms of two

components. First the coordinate system is defined as cartesian, with the positive z-axis serving as the direction of propagation of the laser light and the electric field vector limited to the x-y plane. Polarization of an electromagnetic field is described by the orientation of the electric field vector. Any plane polarized wave can be described in this coordinate system as a superposition of two electric field vectors[5]:

$$\mathbf{E}_x(z,t) = \hat{i}E_{0x}\cos(kz - \omega t) \tag{5}$$

$$\mathbf{E}_y(z,t) = \hat{j}E_{0y}\cos(kz - \omega t + \epsilon) \tag{6}$$

These are simply the x-axis and y-axis components of the total electric field vector. The ϵ term denotes a phase difference between the two components. The total electric field vector can be described by a summation of these two components. For circularly polarized light phase difference is $\epsilon = -\pi/2 + 2m\pi$ where m is an integer. This means that the two components are orthonormal to one another. In addition, E_{0x} = E_{0y} = E_0, making the polarization circular. Our total electric field vector can now be described as[5]:

$$\mathbf{E} = E_0[\hat{i}\cos(kz - \omega t) - \hat{j}\sin(kz - \omega t)] \tag{7}$$

This vector rotates in a counter clockwise direction and is called left-circularly polarized. Had the y component been added, this vector would rotate in a clockwise motion making it right-circularly polarized. If a particle absorbs a photon with a circular polarization, it will also gain the angular momentum belonging to the photon. This gain of angular momentum is considered an energy transition of the angular quantum number m. [5] In the case of our system this will involve a transition of an electron from m = -1/2 to m = +1/2 or visa versa, depending on the spin state of the electron and the direction of polarization of the photon being absorbed. In order for this transition to occur, the photon must have an opposite spin direction from the absorbing electron. As stated by quantum mechanics, if the spin states are the same between a photon and a particle, that photon cannot be absorbed by the particle.

2.4 Optical Pumping and Polarization by Spin Exchange

Optical pumping is a process by which the natural population spin distribution of a uniform gas is changed by adding energy to the system with laser light. This process takes advantage of the Zeeman effect, in which the spin associated with the quantum number m is split by a uniform magnetic field between +1/2 and -1/2. In this case, Zeeman splitting occurs in the valence electron of Rb within the cell. The relative populations of m = +1/2 (spin up) and m = -1/2 (spin down) in a uniform magnetic field are nearly equal. Adding angular momentum with circularly polarized light changes the population ratio which in turn produces a net polarization. This polarization is maintained with the help of Nitrogen(N_2) within the cell. N_2 allows the polarized ^{3}He to relax back down to the ground state through kinetic interactions rather than spontaneous emission of photons. This is important because unpolarized photons emitted spontaneously can substantially contribute to a fast depolarization of the Rb. This process can successfully create a large population of Rb atoms with electrons possessing spin values oriented in the same direction.[7]

Spin exchange is the property used to transfer the polarization of one gas to another. This process involves the hyperfine-like (spin-spin) interactions between two particles. For the purpose of this project, the polarization of valence electrons in Rb will be used to polarize the spin of valence electrons in K, which will then polarize the ^{3}He nucleus. This is done because it is much more difficult to polarize ^{3}He with Rb than it is to polarize it with K. The reason Rb is used at all, is that the laser we have does not operate at the wavelength needed to optically pump K. Since the average polarization of K will be nearly constant after a significant duration of time into the optical pumping process, the final polarization of ^{3}He becomes:

$$P_{He} = \frac{\gamma_{SE}}{\gamma_{SE} + \Gamma} \langle P_K \rangle \tag{8}$$

Where P_{He} is the final polarization of ^{3}He, γ_{SE} represents the rate of spin exchange

between K electrons and helium, $\langle P_K \rangle$ is the average polarization of K valence electrons, and Γ is the total depolarization rate. The spin exchange rate is directly proportional to the concentration of polarized K atoms within the cell.

2.5 Electron Paramagnetic Resonance

NMR measurements are only capable of giving a relative polarization of ^{3}He. This is not useful in determining a reportable value of polarization when characterizing the cell. In order to obtain an absolute polarization, a reference point or comparison is needed. Early on in cell characterization the polarization of water was used to calibrate NMR data in order to obtain an absolute polarization measurement. This method was unreliable since the polarization of water is very low and hard to detect. Electron Paramagnetic Resonance (EPR) is a much more effective method of obtaining absolute polarization because the signal is easier to obtain since each Rb atom could emit an EPR photon that can be collected. The population of Rb is large enough within the cell to create a large EPR signal.

EPR takes advantage of the hyperfine splitting which occurs between the valence electron of Rb and the Rb nucleus. This causes an energy split, which is further split by an external magnetic field. During the polarization process, the Rb electron oscillates between two dominant energy levels. The EPR resonance frequency is the frequency at which this transition occurs. By adding a coil to the system which is driven at the EPR resonance frequency, the energy transition of the Rb electron can be induced. When the electron is re-polarized by laser light, a small percentage of Rb valence electrons emit light at one of two possible frequencies. One of these frequencies is identical to the laser frequency(D_1) while the other is not(D_2). D_2 light is measured by a photodiode. When the magnitude of this signal is highest, resonance has occurred, indicating a maximum number of electrons making a transition.[4]

Once the EPR frequency(Δ_{EPR}) is found, polarized ^{3}He is flipped via Adiabatic

Fast Passage(AFP). AFP is explained in more detail in Section 3.4. The flipping of ^{3}He spins causes a shift in EPR frequency due to the polarized ^{3}He. This frequency shift is directly related to the polarization percentage of ^{3}He. The EPR frequency shift due to polarization is[4]:

$$\Delta\nu_{EPR} = \frac{2\mu_0}{3}\frac{d\nu_{EPR}}{dB}\kappa\mu_{He}\eta_p P_p \tag{9}$$

This can be manipulated to calculate polarization from the EPR frequency shift:

$$P_p = \frac{3\Delta\nu_{EPR}}{4\mu_0\frac{d\nu_{EPR}}{dB}\kappa\mu_{He}\eta_p} \tag{10}$$

In these equations P_p is the polarization percentage of Rb valence electrons, μ_0 is the magnetic permeability of free space, $\frac{d\nu_{EPR}}{dB} \approx 4.67$ x 10^3 MHz/T, $\mu_{He} = 1.07$ x 10^{-26}J/T, and $\kappa = 4.52 + 0.00934T_p$, where T_p is pumping chamber temperature.[4] The value of η_p is governed by the equation[4]:

$$\eta_p = \frac{\eta_0}{1 + \frac{V_p}{V_t}\left(\frac{T_p}{T_t} - 1\right)} \tag{11}$$

where η_0 is the cell density in amagats, T_p and T_t are the temperatures of the pumping and target chambers respectively, and V_p and V_t are volumes of the pumping and target chambers respectively.[4]

3 Experiment

3.1 Laser Studies

At the start of the project, a functioning monochromator had already been constructed by a graduate student. The monochromator was capable of taking broad bandwidth laser light and sweeping through the narrow bandwidth range of frequencies at with acceptable accuracy. A new spectrometer was used to determine the frequency range and narrow bandwidth of the monochromator used in conjunction

with a broadband diode laser. The laser used had a bandwidth of about 2nm and a maximum power output of 30W and a output frequency peak at 795nm. This laser was directed to the lab area with a multimode 800μm core diameter fiber. The laser light emitted from the fiber was highly divergent. The first goal of the project was to change the fiber output to a highly collimated beam with a small beamspot. The first measurement made to meet this goal was to map the profile of the laser output from the fiber. This was accomplished by creating a data set relating power output of the laser to the radius of the beamspot. The setup for this measurement is illustrated in Figure 5. A fiber, thermal receiver, and iris were mounted at fixed positions. The

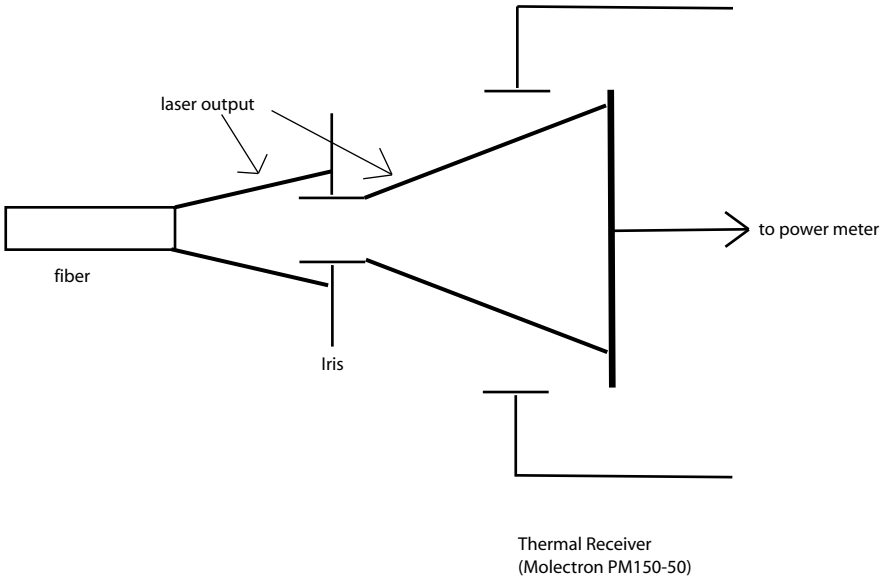

Figure 5: This is the experimental setup used to map the profile of the laser output straight from the fiber. In the setup used to generate the data in Figure 6, the fiber was fixed 4.6cm from the iris and 16.2cm from the thermal receiver.

positions were picked so that a completely open iris would allow all of the light emitted by the fiber to be captured by the receiver. Since the laser used operated at a peak intensity frequency of 795nm, the total power of the laser was read by a thermal receiver, which takes the heat integrated over its entire surface and converts it to a voltage to be amplified and converted to a power by the power meter. The iris was then closed to a small diameter and gradually increased. The increase in diameter was made with the calipers used to measure the aperture diameter, this allowed an accurate measurement of the diameter without changing it due to caliper pressure. After each increase the power was recorded. Finally a plot was made relating iris diameter to time. This plot was fit to the gaussian curve (given in Equation 1). In this fit, the variables outside of the brackets were considered to be one parameter, P_0. When fitting the data, the variables P_0 and $\omega(z)$ were free parameters. The R value of this curve gave a reasonable assessment as to whether or not the laser profile was gaussian in nature. This data is displayed in Figure 6. The function used to fit this data is:

$$f(r) = AB^2 \left(1 - exp\left(-\left(\frac{r-C}{B}\right)^2\right)\right) \tag{12}$$

Where A represents the suppressed constants in Equation 1, B represents the beam waist at a given point along the axis of propagation (represented by $\omega(z)$ in Equation 1), and C accounts for a linear offset. Figure 6 indicates that the laser light emitted from the fiber has gaussian behavior. In other words, we can conclude that the laser is a gaussian laser which is essential information to have before attempting to change the laser light behavior.

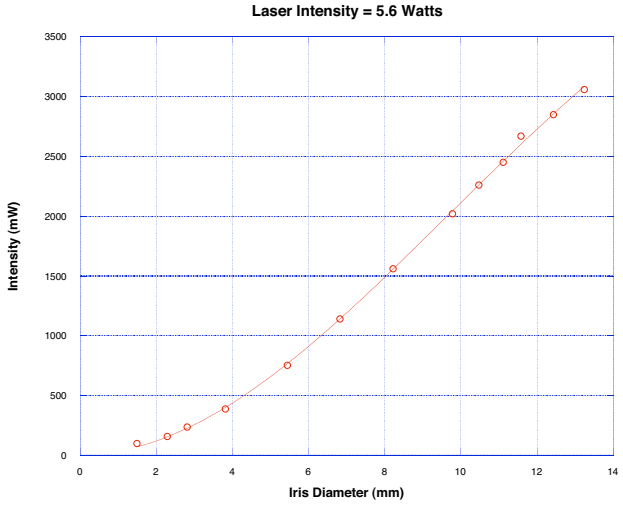

Figure 6: This is the data taken of the intensity profile of the laser emitted from the fiber. In the fit m1, m2, and m3 correspond to A, B, and C respectively in Equation 12. The R value is very close to 1, which indicates a good fit.

3.2 New Oven System

A new oven system was constructed in order to handle a higher temperature as well as a larger cell design. This new oven system is mainly constructed from glass mica and 316 stainless steel. This new oven is shown in Figure 7. This type of stainless steel is necessary because it is non-magnetic. Any magnetic materials in close proximity to the oven would make any NMR measurements impossible. In order to accommodate the new oven, a new apparatus was needed to mount the oven and protect the lab from heat and possible explosions. This was a large part of my focus in the spring.

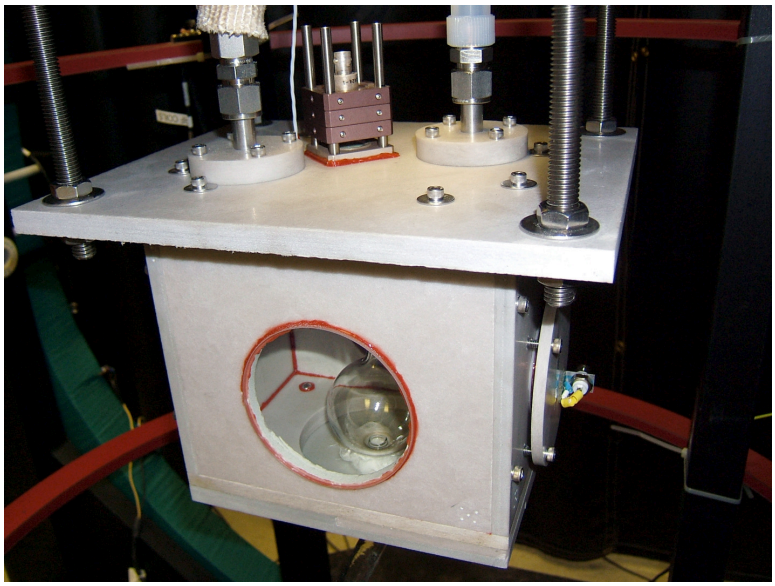

Figure 7: This is the new oven used to polarize ^{3}He. It is composed mainly of a ceramic glass mica. The hardware is all 316 stainless steel(non-magnetic). The oven hangs from a composite top piece capable of tolerating the high temperatures necessary to polarize a hybrid Rb/K cell while still remaining rigid. The rods used to hang the cell are the large corner rods depicted in this figure. The oven is being shown with a dummy cell mounted to give an idea of how the cells will fit in the oven.

The oven was mounted from a dense composite material which was both rigid and

heat resistant. This top piece was fitted into the fiberglass posts that secure the main and RF coils. The oven was then mounted by hanging it from the top piece with 316 threaded steal rods. The oven height was calibrated and fixed. The coil table serves as a surface for mounting the NMR pickup coils. In the new design, rather than bolting the coil table into the fiberglass posts, rails were installed so that the coil table could be slid in and out with ease. This allows us to mount and remove cells while leaving the oven in a fixed position. This change was necessary since the new oven weighs over 50 lbs, making it impossible to mount alone and difficult even with two people. The top piece and coil table are shown in Figure 8.

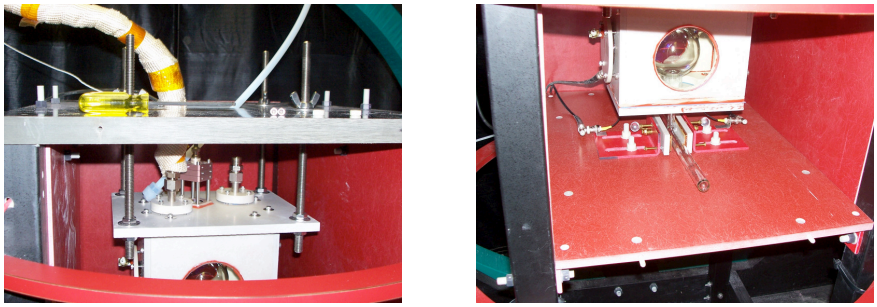

(a) Top piece used to mount the oven

(b) Coil table with NMR coils mounted

Figure 8: The coil table and top piece of the new system. The top piece holds the oven in place at the calibrated ideal height. The coil table rests on rails. This allows the coil table to be slid out of the system so that a cell can be mounted into the oven without changing the height of the oven.

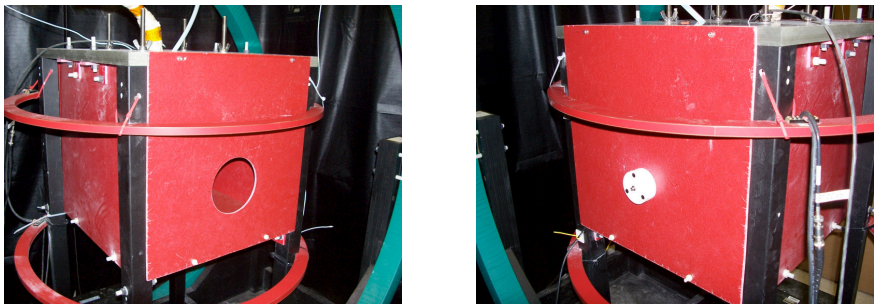

(a) Front (b) Back

Figure 9: This is the polarization system with the blast shield in place. The blast shield effectively protects the lab and researchers in the event that a cell explodes during the polarization process.

An effective blast shield is needed in the event that the cell explodes under the high temperature and energy it is exposed to. Cells used in this experiment contain high pressure gas, with pressures between 6 and 10 atmospheres. Without an effective protective shield around the oven, an explosion could heavy damage to surrounding equipment or cause serious injury to researcher. I designed panels to serve as a protective shield. They were machined from fiberglass sheets about 1/8" thick. The front panel has a hole to allow laser light to get to the oven. The back panel has a photodiode installed for later uses in EPR measurements. The fiberglass material possesses the tolerances necessary to withstand the high temperatures of the oven while at the same time providing effective protection from glass shards or ceramic components that may be ejected during an explosion. The completed apparatus is

shown in Figure 9.

3.3 Setbacks

There were many setbacks throughout the project which hindered progress. The main underlying problem to overcome with the new cell design was the high temperature and pressure needed within the oven. When first heating up the oven, a component in the top plate of the oven expanded, causing the plate to crack. Later, heating tests were resumed and it was discovered that the oven was unable to reach the desired 230°C necessary to polarize the hybrid cells. This required the old heating system to be upgraded. I added a new 750 watt air heater to the system. This is a simple heater which uses electric current resistance to heat air that passes through it. Once a new heater was integrated into the heating system, more heating tests were performed to see if the oven could reach the desired temperature. It was soon discovered that the pressure inside the oven due to heating was too high. An optical lens mounted into the top oven was ejected during the first attempt to heat up the oven with the new heating system, destroying a neutral density filter. Once the lens was re-secured further heating tests caused the back window of the oven to breach. Eventually it was concluded that the hose used to relieve pressure from the oven was too thin, causing too much pressure to build up inside the oven. This hose was removed, allowing the oven to vent directly into the room. This could cause future problems with the laser system and electronics, since the room becomes very hot during experiment. A new pressure relief system must be constructed that can effectively direct air away from the lab without causing a high pressure buildup within the oven.

3.4 Polarimetry

Polarimetry is the measurement of the amount of polarization of a fixed number of particles. This value can be found through the process of nuclear magnetic resonance (NMR). This process involves flipping the spins of the polarized ^{3}He atoms isentropically in a process known as Adiabatic Fast Passage(AFP). AFP flips the spins of ^{3}He slow enough to cause an adiabatic process but fast enough to ensure that the ^{3}He spins don't relax back down to the ground state.

The system used to accomplish this is illustrated in Figure 2. The main coils in this system provide a uniform magnetic field along the axis of polarization. They are mounted on either side of the oven system and are the large vertical coils labeled in Figure 2. The RF coils produce an oscillating magnetic field at an adjustable frequency. These are the smaller horizontal coils depicted in Figure 2. A 795nm laser is used to polarized Rb in the cell; the laser light is circularly polarized and directed into the target cell. A third pair of coils, called pickup coils, are mounted to either side of the cell and are used to pick up a current when the polarization of ^{3}He switches and a magnetic flux is produced. NMR uses RF coils, pickup coils, and main coils together. With the RF coils kept at a constant frequency, the main coil magnetic field is increased to pass through resonance. The process is kept isentropic by keeping the rate of change in magnetic field strength due to the main coils low. This change in polarization induces a current on the pickup coils in turn introducing a voltage to be amplified and recorded by electronics. The peak voltage induced is proportional to the polarization of the ^{3}He within the cell.

The NMR system will give a good value for polarization, but this will only be a relative polarization since a reference point is needed with which to compare it to. NMR can calibrated using a technique known as Electron Paramagnetic Resonance (EPR). This process measures the shift in electron energy levels when placed in a magnetic field. There are many sources of magnetic fields which cause this energy

split in our system. Aside from the coils, both the polarized ^{3}He and the spin exchange interactions present in the system affect the energy levels of the alkali electrons.

3.5 NMR Measurements of Cell "Dale"

After the polarizing system was built, NMR coils were wound and mounted to the coil table. We mounted a pressurized ^{3}He cell and used the new system to perform NMR measurements on it. Since NMR measurements have already been performed on this cell with the old system, data obtained with the new system could be compared to parameters previously calculated.

The glass cells used in the system all have similar design. Each glass cell consists of a spherical pumping chamber which contains the alkali vapor. This chamber is where the hybrid alkali gas is polarized by laser light. This polarization is transfered via spin exchange to ^{3}He mainly concentrated in a cylindrical chamber below the pumping chamber. At Jefferson Lab accelerated electrons are directed into this chamber and scattered from polarized ^{3}He inside of it.

The cell "Dale" was mounted into the cell mount component of the oven using a high temperature adhesive known as RTV. The height of the cell above the mount was calculated so that the pumping chamber would be centered in the window of the oven. The coils were then placed as close as possible to the cell without touching it. Then with the main coils and RF coils on, the NMR coils were adjusted to be parallel to the cell. Signal from the NMR coils is displayed on two channels of the oscilloscope, each representing a cartesian axis. When the coils are parallel to the cell, the signal will be minimized on the one axis while minimized on the other. With the main and RF coils operating, the NMR coils were adjusted until this condition was met. Once the coils were aligned, the oven system was brought up to 230°C and the laser system was activated. The laser system consists of three 30W lasers with a peak frequency of 795nm. All lasers are circularly polarized and directed into the

pumping chamber.

The characterization of "Dale" consisted of three major measurements. One, called the spin up measurement is a plot of the polarization process as the cell is being polarized. This was established by performing NMR measurements periodically as the cell was polarizing. The second measurement is an AFP loss measurement. This is performed after the cell reaches peak polarization. The purpose of this measurement is the establish the amount of polarization lost with each Adiabatic Fast Passage sweep. This measurement involved five NMR sweeps done in short succession with the laser system turned off. This yielded a correction factor used in the third calculation and ultimately the calculation of the lifetime of the cell. The third measurement performed is a plot of the spin down process. This measurement consists of a series of NMR sweeps with the laser system and heating system off. This allows us to accurately plot the relaxation of the cell to an unpolarized state. The spin up measurement is used to calculate the maximum polarization of the cell and the spin up time. The AFP loss measurement is used to establish a spin down correction factor. The spin down measurement is used to calculate the relaxation time of the cell.

3.5.1 Spin Up Measurement

The spin up data for "Dale" is displayed in Figure 10. This data was taken with the target oven held at 230°C and all three lasers directed into the pumping chamber. The NMR Signal corresponds to a net polarization of ^{3}He within the cell. A higher signal indicates a higher flux induced when the polarization is flipped via Adiabatic Fast Passage. As indicated in Figure 10, the polarization has an exponential relationship to time. From the data obtained from the exponential fit, two parameters can be determined. One is the maximum NMR signal of the cell, while the other is a polarization time. Polarization time is the amount of time it takes the cell to reach a polarization $\frac{1}{e}$ less than the maximum polarization.

The exponential equation used to fit this data is:

$$F(t) = I_0 \left(1 - e^{-\frac{t-B}{C}}\right) \tag{13}$$

where I_0 is the maximum signal at saturation, B is a fitting parameter, and C is another fitting parameter determined by the fit. The fitting parameters B and C are used to calculate a Spin Up time. According to the fit in Figure 10, the maximum signal I_0 has an average value of 71.21mV. In earlier fits of Dale performed with the old system, I_0 was fitted to a value of only 60mV. While EPR was not performed with the new system on "Dale," this value suggests that a higher polarization of "Dale" was achieved with the new system. The polarization time was calculated by manipulating Equation 13 and with a value of $I_0 \left(1 - \frac{1}{e}\right)$ used for the function solution. This manipulation is:

$$t = B + C \tag{14}$$

The parameters for B and C were obtained from the fitting functions displayed in Figure 10. Since B is a linear offset, the polarization time of the cell is simply the parameter C. The average time between the Up Sweep and Down Sweep was calculated to be 8.67 hours. This is number is significantly lower than parameters obtained with the old system on "Dale." Figure 10 clearly demonstrates the exponential relationship between time and NMR signal. R values on both curves are ≈ 1. This indicates a strong similarity between the fitting curve and the data.

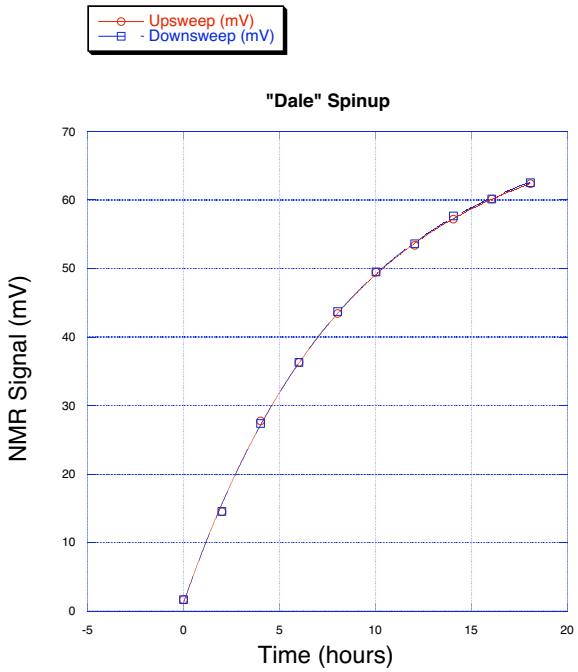

Figure 10: This graph represents the data obtained during the Spin Up process in which the ^{3}He cell was polarized. The parameters in the red box represent the sweep of the B field up from 25G to 32G while the parameters in the blue box represent the sweep of the B field down to 25G from 32G. Numbers were calculated using both sets of parameters and then averaged in order to eliminate random error.

3.5.2 AFP Loss Measurement

The purpose of the AFP loss measurement is to determine how much of the original polarization is lost to the actual signal induced on the NMR coils. Since the computer system used to make NMR measurements documents data to the nearest minute, an AFP loss calculation dependent on time would be inaccurate. Instead, an AFP loss calculation dependent on sweep was established. In other words, an amount of signal lost per sweep was calculated. The data for this measurement was obtained by performing five NMR sweeps consecutively soon after the lasers were turned off. This would give an accurate plot of signal loss without the laser light present to repolarize the gas. The data obtained for this measurement is displayed in Figure 11.

The AFP Loss data was fit to a linear function. The average slope of the two fits gives an average loss of signal per measurement. This yielded a correction factor of 0.102 mV of polarization lost per sweep. Dividing this rate by the initial signal voltage at $t = 0$ give a percentage of signal lost. The average percentage of signal lost was 0.16%. It is clear in Figure 11 that the data obtained during the AFP Loss measurement was not well behaved. This could be due to NMR sweeps occurring too close to one another. In future AFP Loss measurements the sweeps should be performed further apart from one another. For this measurement, the time interval between sweeps was programed to be 6 seconds. An AFP Loss measurement performed on "Dale" with the old system used a time interval of 30 seconds. This data was much better behaved. For future AFP Loss measurements, a time interval of 30 seconds would be more appropriate. The AFP Loss correction factor will be used in the Spin Down measurement. Since the Spin Down process will be documented by repeated NMR Sweeps, there will be a significant loss of polarization due to frequent NMR Sweeps. To correct for this, a linear correction factor is introduced to the Spin Down data in order for a more accurate calculation of cell polarization lifetime.

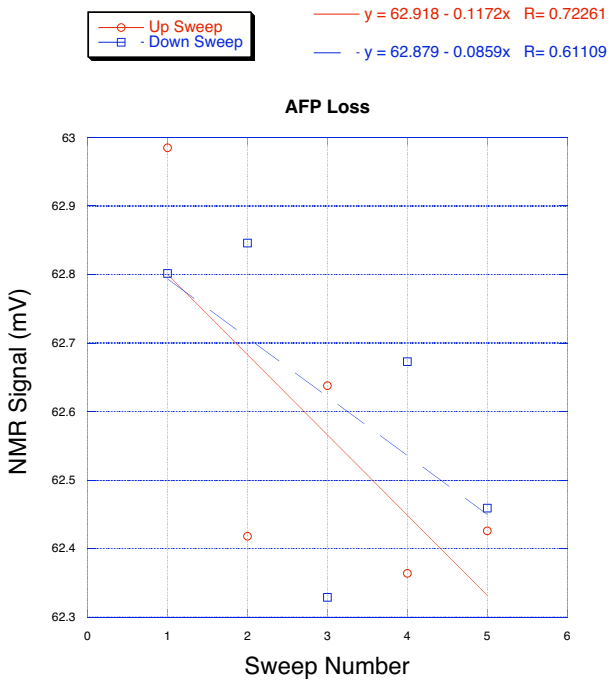

Figure 11: This graph represents the data obtained during the AFP Loss measurement. The parameters in the red box represent the sweep of the B field up from 25G to 32G while the parameters in the blue box represent the sweep of the B field down to 25G from 32G. Numbers were calculated using both sets of parameters and then averaged in order to eliminate random error.

3.5.3 Spin Down Measurement

This spin down measurement is important for calculating the lifetime of a cell. The cell lifetime is defined as the amount of time it takes the cell to drop to a factor of $1/e$ of its maximum polarization. This parameter is essential for approximating the amount of polarization left in the cell after a given amount of time has elapsed which is needed for as a parameter for electron scattering experiments performed at Jefferson Lab. The AFP Loss correction for each data point is simply the factor determined in the AFP Loss measurement compounded at each data point. This means that for each consecutive correction, we must add in the old correction:

$$f(\delta) = \text{Signal} \cdot \delta + \Delta \tag{15}$$

Where Δ represents the AFP correction of the previous data point and δ represents the AFP correction factor calculated earlier to be 0.16%. This equation was used to calculate corrected Spin Down data. Figure 12 displays both the original Spin Down data as well as the corrected Spin Down data. The equation used to fit the data in Figure 12 is:

$$f(t) = I_0 e^{-\frac{t-C}{B}} \tag{16}$$

Solving for t:

$$t = B \ln\left(\frac{I_0}{f(t)}\right) + C \tag{17}$$

Plugging in f(t) = $I_0 \frac{1}{e}$:

$$t = B + C \tag{18}$$

Where B is the lifetime of the cell since C is a linear offset. Given the parameters found in Figure 12, the lifetime of the cell was calculated to be 37.04 hours. This was determined by calculating the lifetime using parameters from the corrected Sweep Up curve as well as the corrected Sweep Down curve and finding an average between the two to reduce random error. The calculated lifetime of the cell is substantially

larger than the previously calculated lifetime of 15.3 hours. This is not significantly attributable to the new polarizing system being implemented. The longer lifetime could simply be a stabilization between the gas and the glass cell due to prolonged interaction. The cell "Dale" was in storage for over a year before it was tested again in the new system. Improved cell characteristics could simply be due to long lasting stable conditions.

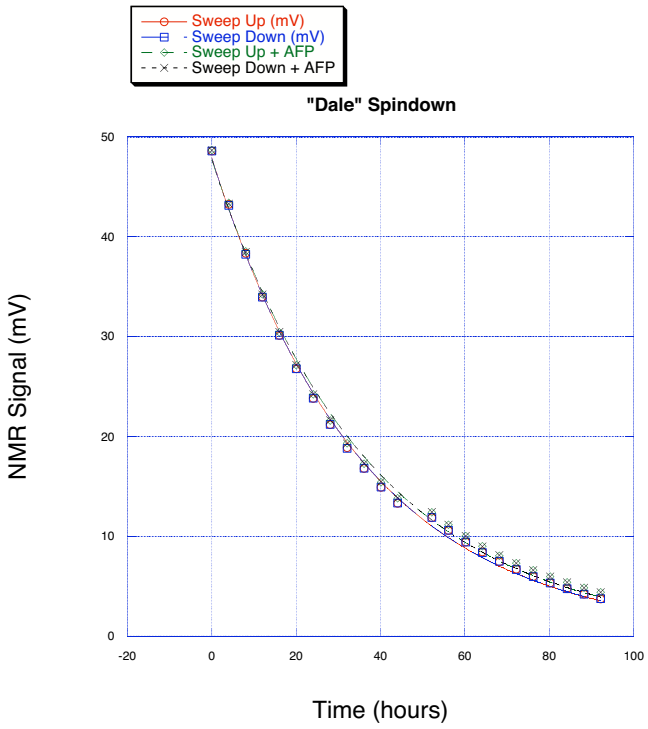

Figure 12: This graph represents the data obtained during the Spin Down measurement. The parameters in the red box represent the sweep of the B field up from 25G to 32G while the parameters in the blue box represent the sweep of the B field down to 25G from 32G. Numbers were calculated using both sets of parameters and then averaged in order to eliminate random error.

3.6 NMR and EPR Measurements of Cell "Aaron"

In addition to a previously tested cell "Dale", the new system was used to characterize an untested cell, "Aaron." The same measurements that were performed on "Dale" were also performed on "Aaron." The characterization of "Aaron" was very important not only because we did not have data on it yet, but also because the cell design of "Aaron" was untestable with the old system. This limitation was due to the large volume of the pumping chamber of "Aaron" and other cells like it. The old oven was not large enough to accommodate such a large pumping chamber. The new polarization system was used to obtain a polarization time, cell lifetime, and an absolute polarization measurement made possible by EPR. The Spin Up measurement was interrupted by two problems. The first problem was minor. The heating system has a shutoff temperature built into it. This will turn off the heating system if the oven temperature becomes too high. The preset temperature threshold was originally 240°C. At some point the oven reached this temperature and the heating system was automatically shut off. This interrupted the Spin Up process. The threshold temperature was reset to 250°C and the Spin Up process was restart. The second problem encountered during the Spin Up process was much more serious. For reasons currently unknown, one of the three lasers used to polarize the cell stopped working. This could be due to a variety of reasons including feedback or simply overuse. We were unable to get the laser up and running again, forcing us to polarize with only two out of three lasers functioning.

The data obtained from the Spin Up measurement is displayed in Figure 13. The maximum polarization of "Aaron" was calculated to be 42.75%. This is substantially lower than the similar parameter calculated from "Dale" but it is understandable since one of the lasers stopped functioning. The spin-up time of "Aaron" was calculated to be ≈ 4.93 hours. The data obtained from the Spin Down measurement is displayed in Figure 14. The lifetime of "Aaron" was calculated to be ≈ 12.02 hours. This

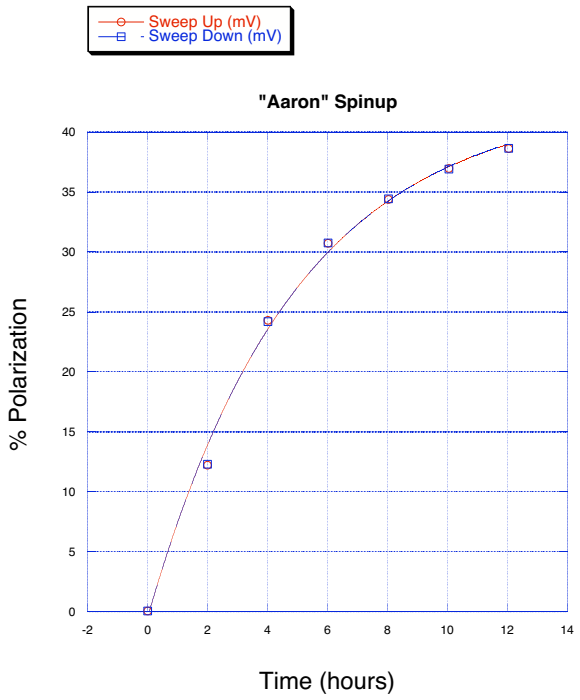

Figure 13: This is the Spin Up data taken during the polarization process of the cell "Aaron." The polarization time was calculated by using the same relations derived for measurements taken on "Dale."

parameter is similar to the original lifetime calculated for "Dale." Since the lifetime of "Dale" improved between characterizations it is reasonable to assume that "Aaron" will exhibit a similar improvement later on.

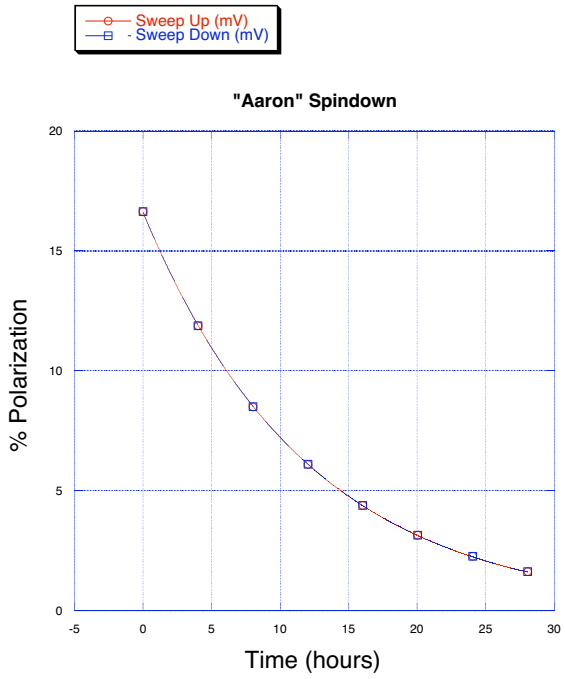

Figure 14: This is the Spin Down data taken of the cell "Aaron." The cell lifetime was calculated by using the same relations derived for measurements taken on "Dale."

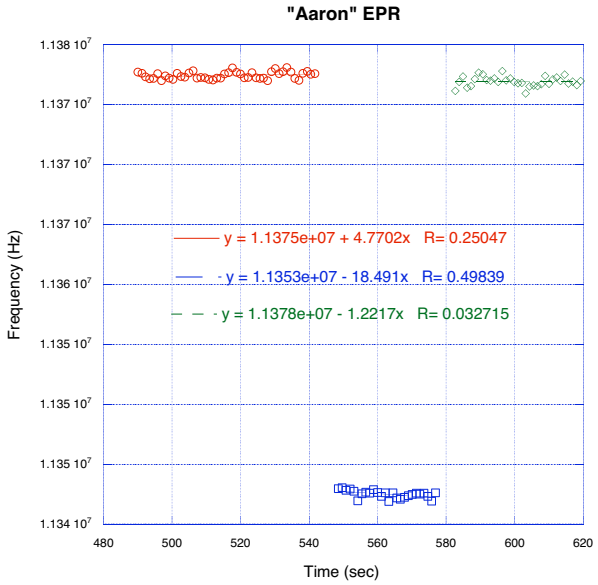

Figure 15: This is the EPR signal analyzed to calculate the absolute polarization of "Aaron." The net frequency shift is calculated from the linear fits and is used among other parameters for the calculation of absolute polarization of ^{3}He in Aaron. In order for the EPR data to be analyzed, three linear fits were applied to each line and used to find an average value of the line.

The EPR signal for the cell "Aaron" is displayed in Figure 15. The net frequency shift calculated from data displayed in Figure 15 is proportional to the magnitude of polarization of ^{3}He in the cell. A total frequency shift of 34.775 KHz was calculated from the data. This yielded an absolute polarization of 32.57%. This would be considered low under normal circumstances but since only two lasers were used to polarize "Aaron" the polarization achieved is adequate. Immediately after EPR data was taken, an NMR sweep was performed. The peak intensity of the NMR sweep was used in conjunction with the calculated absolute polarization to obtain a calibration constant:

$$\alpha = \frac{P_p}{I_0} \tag{19}$$

Where P_p is the absolute polarization given by the EPR measurement and I_0 is the maximum signal intensity of the NMR sweep performed after the EPR measurement. The calibration constant for "Aaron" was found to be $\approx 1.0\%/\text{mV}$. Any NMR signal for "Aaron" can be converted into a polarization with the following relation:

$$\text{Signal} \cdot \alpha = P_p \tag{20}$$

Where Signal denotes the NMR signal to be converted and α is the calibration constant calculated with the previous equation.

4 Conclusions

4.1 Laser Study

The data displayed in Figure 6 very closely fit a gaussian distribution with an R value ≈1.0. With this in mind, we then attempted to find a method for manipulating the fiber output into a beam that had a beamspot diameter at the monochromator less than 5mm but did not double over the distance of four meters. Using geometric optics calculations we used the invariant mentioned in Equation 19 and determined that the tolerances mentioned could not be achieved with conventional spherical optics. With the possibility of geometric optics ruled out, we then investigated the possibility of using aspherical optics, which are designed to correct for spherical aberrations. After consulting with Thor Labs, we discovered that aspherical optics could not achieve the beam waist and far field divergence we needed due to the properties of the cable used to direct the fiber from the laser to the optical table where the monochromator is built. The fiber used is a multimode fiber and has a wide core diameter of 800μm. A multimode fiber is required with the use of this laser because the light it emits is composed of a series of diode lasers all shunted into one fiber. To obtain total internal reflection of the fiber necessary to avoid damaging the components of the laser, the use of a wide core multimode fiber is required. Since lenses are only capable of imaging the core of a multimode fiber, only conventional geometric optics would be able to obtain the laser properties we wanted. We have concluded that this would not work, so we decided to pursue a different direction in the project.

4.2 Polarization Measurements

The NMR measurements performed on the cell "Dale" told us a variety of things about the new system as well as the cell. The Spin Up measurement yielded a lower

polarization time than previously calculated. This tells us that the new polarization system is capable of polarizing our cells at a faster rate. While the data for the AFP Loss was not too well behaved, it still gave a linear relationship between NMR sweep and signal loss. The Spin Down measurements gave a much improved cell lifetime providing a more up to date characterization of Dale's parameters.

The successful characterization of "Dale" proves that the new NMR system successfully polarizes ^{3}He cells and yields better parameters than the old system. This is due to a higher oven temperature achieved by the new oven design as well as a new NMR coil design, which is easier to adjust for calibration purposes. The new heating components that I added to the heating system make this higher temperature possible. This new system will function well for the polarization of higher volume Rb/K hybrid cells.

The new system was also successful in characterizing a new type of cell with a large pumping chamber ("Aaron"). The new system was built to accommodate cells of this design. Characterizing "Aaron" was crucial in establishing how successful this endeavor was. In spite of the major setback of a broken laser, resulting in the loss of one third of the polarizing light, we were still able to polarize "Aaron" and obtain an absolute polarization of 32.57%.

Problems with the new system still remain, which is typical for any new system. The pressure problem should be addressed first. In the old polarization setup, an air hose was attached to the top plate of the oven for the purpose of relieving pressure buildup within the oven. This hose transported hot air from within the oven to outside of the lab. After many setbacks that occurred during initial heating tests, we decided that the pressure relief hose diameter was too small. The pressure inside of the oven became too large and breaches occurred. For this reason, we detached the pressure relief hose, causing hot air to be dumped directly into the lab. This could cause problems for the laser system as well as various other components within the

lab that are susceptible to overheating. The two possible solutions to this problem are either a more secure oven window design or a wider pressure relief hose. The old oven design included clamps which fit over the oven windows establishing a much more secure window design. The ideal solution would be to pursue both possibilities. This would involve installing window clamps as well as a larger pressure relief hose. The problem with installing window clamps would be the added machining that would be needed to do so. The glass mica material is exceedingly difficult to machine. This would be a timely and costly solution but would carry with it a lower possibility of oven failure.

The new polarizing system is better equipped to handle larger volume hybrid ^{3}He cells. This project has thoroughly investigated the implementation of a new density evaluation system and has been instrumental to the construction and operation of the new polarization system. With a few minor adjustments to the system it will be ideal for polarization and characterization of hybrid Rb/K ^{3}He cells.

References

[1] Gaussian beam. Webpage - *http* : *//en.wikipedia.org*, November 2006. This is a website containing general information about gaussian beams.

[2] Lens (optics). Webpage - *http* : *//en.wikipedia.org*, November 2006. This a website containing general information about lens optics.

[3] Polarized Helium-3 Target Lab at The College of William and Mary. $Webpage - http : //pol3he\_daq.physics.wm.edu/\ pol3he/Index/$, April 2007. This the main website for Dr. Todd Averett's Polarized ^{3}He Lab.

[4] E.M. Buckley. Measuring the Polarization of a ^{3}He Target Cell Using Electron Paramagnetic Resonance. Senior Thesis - College of William and Mary, 2005.

[5] E Hecht. *Optics - Fourth Edition*. Addison Wesley, 2002.

[6] P.A. Mastromarino, C.R. Otey, D. Pripstein, and E.W. Hughes. Tunable diodle laser study of pressure broadening of Rb D_1 lines in the presence of ^{4}He buffer gas. *Nuclear Instruments and Methods in Physics Research B*, 194:69–77, 2002.

[7] D.E. Milkie. Polarization and Polarimetry of ^{3}He. Senior Thesis - College of William and Mary, 2002.

[8] J Singh, V.V. Neiyubin, M Carl, S Rohrbaugh, and W.A. Tobias. A potpourri of combiner fiber studies. unpublished post doc work forwarded from Jefferson Lab, 2005.